Published in final edited form as:
Adv Mater. 2012 July 24; 24(28): 3831–3837. doi:10.1002/adma.201103550.

Plasmonic nanobubbles enhance efficacy and selectivity of chemotherapy against drug-resistant cancer cells

Dr. Ekaterina Y. Lukianova-Hleb
Departments of Biochemistry and Cell Biology Rice University, Houston, TX 77005 USA

Dr. Xiaoyang Ren
Department of Head and Neck Surgery The University of Texas MD Anderson Cancer Center, Houston, TX 77030 USA

Dr. Joseph A. Zasadzinski
Chemical Engineering and Materials Science University of Minnesota, Minneapolis, MN 55455 USA

Dr. Xiangwei Wu
Department of Head and Neck Surgery The University of Texas MD Anderson Cancer Center, Houston, TX 77030 USA

Dr. Dmitri O. Lapotko*
Departments of Biochemistry and Cell Biology Department of Physics and Astronomy Rice University, 6100 Main, MS-140 Houston, TX 77005 USA

Keywords

gold nanoparticles; plasmonic nanobubbles; cancer; Doxil; drug resistance

Oral cavity squamous cell carcinoma (OCSCC) is one of the most prevalent malignancies affecting patients worldwide.[1] Advanced OCSCCs are at high risk for local recurrence and are associated with poor prognosis.[2] The major reasons for this are 1) incomplete removal of cancer cells by surgery, especially when complicated by micro metastasis and co-localization of cancer cells with functionally or cosmetically important structures; 2) multi-drug resistance of cancer cells, and 3) acute and long-term toxicities of radio- and chemo-therapies. Therefore, new treatment strategies are needed to provide cell level selectivity of cancer treatment and high efficacy against drug-resistant cells for OCSCC and other superficial cancers.

By themselves, NPs[3] can destroy cancer cells via hyperthermia by converting optical, radiofrequency and/or magnetic energy into local heating.[4, 5, 6] However, such direct heating methods require significant NP loading, thus limiting selectivity due to the diffusive heating of surrounding tissue. A superior approach is to use NPs to generate plasmonic nanobubbles (PNB), transient vapor nanobubbles generated by short laser pulses that superheat gold NPs.[7, 8] The temporally and spatially controlled initiation and collapse of PNBs creates local optical and mechanical effects that can enable imaging,[8] intracellular molecular targeting,[9] localized drug or gene delivery,[10] and selective elimination of cells for therapeutics, theranostics and microsurgery.[11, 12] In addition, the optical and acoustical properties of PNBs provide a mechanism for real-time guidance of their therapeutic

*Phone: 713-348-3708 Fax: 713-348-5154 dl5@rice.edu.

action.[12] PNB also offer improved safety due to their transient, on-demand nature; PNBs do not exist until activated with an optical pulse, then disappear within nanoseconds.

Superficial tumors such as OCSCC are particularly accessible for topical application of NPs, drugs and near infrared optical energy, presenting an ideal platform to develop combined PNB-drug therapy. In this communication we focus on the cell-level mechanisms based on the effects of antibody-labeled gold NPs, focused and pulsed NIR light, anti-cancer drugs and PNBs in an *in vitro* model of OCSCC. Our goal is to develop an efficient therapeutic mechanism that will selectively overcome drug-resistance of cancer cells while reducing the non-specific toxicity of standard chemotherapies.

To achieve cancer cell specific formation of NP clusters (Fig. 1A), the NP - antibody conjugate type, concentration and incubation time were optimized for maximal selectivity of NP clustering in cancer cells (red in Fig. 1B). The size of an NP cluster was measured in individual cells through the maximal pixel amplitudes of the scattering image (Supporting Information, Fig. S1). Laser wavelength, fluence and pulse duration were optimized for maximal PNB generation in multiple target cells that were simultaneously exposed to single broad excitation laser pulses that simultaneously irradiated hundreds of mixed target and normal cells (Fig. 1C, D) (Supplementary Information). We determined that near infrared (NIR)-absorbing gold nanoshells conjugated to Panitumumab antibodies formed NP clusters selectively in cancer cells through EGFR (Epidermal Growth Factor Receptor that is over-expresses in cancer cells) -mediated endocytosis in 24 hours under a reduced NP load that minimized NP cluster formation in normal cells (Fig. 1B). These NP clusters provided cancer-cell specific generation of PNBs under low optical excitation fluence, while minimizing PNB generation in adjacent cells without NPs or with single or unclustered NPs.[8, 13, 14]

PNBs were induced in co-culture of cancer and normal cells (Fig. 2A) by single broad NIR laser pulses of wavelength 820 nm at a fluence of 40 mJ cm^{-2}. The 260 μm diameter laser beam (brown circles in Fig. 2A,B) irradiated hundreds of co-cultured normal and cancer cells simultaneously. Generation of PNBs was monitored in individual cells through time-resolved optical scattering imaging (Fig. 1D) and time-responses (Fig. 2A, insert).[7, 8] Cell death levels were measured at 2 and 24 hours, and did not show significant differences. PNBs destroy cells through disruption of the membrane and other structures in an explosive manner that takes less than a second.[12] Most normal cells survived PNB treatment, even those adjacent to cancer cells in which PNBs were generated, showing the extremely localized effects of PNBs. The normal cell death level was 21±8% while 97±3% of cancer cells died after a single pulse treatment (Fig. 2A III, Table S1).

To understand the mechanisms behind the therapeutic selectivity of PNBs, we measured the level of cell death as a function of PNB lifetime (proportional to PNB size[13, 15]). Fig. 3A showed a threshold of 60–70 ns for the onset of PNB-induced cell death, followed by a linear increase in cell death level with PNB lifetime up to 100% cell death at 220–250 ns. The 20 mJ cm^{-2} threshold fluence needed to generate the lethal PNBs was greater than the 15 mJ cm^{-2} threshold required to generate a PNB (Supporting Information, Fig. S2D). This increased threshold for PNB cell-killing activity shows that small PNBs (less than 60–70 ns) do not kill the cells. Observed threshold nature of PNBs allows to discriminate between cancer and normal cells (with higher thresholds for normal cells due to smaller size of NP clusters in them). This property was not found in other photo-induced phenomena associated with plasmonic NPs such as scattering, luminescence, heating, or generation of acoustic waves that do not have any thresholds and therefore cannot discriminate between cancer and normal cells. Cell destruction is controlled through PNB lifetimes, which in turn are determined by the fluence of the laser pulse. The enhanced selectivity of PNB therapy is due

to three multiplicative factors: 1) the largest NP clusters are formed in endosomes in antibody-targeted cells; 2) the threshold fluence for cell death depends on the size of NP cluster, and 3) the energy threshold for PNB formation results in minimal destruction of normal cells.

To compare PNB generation to localized hyperthermia (Fig. 2B), we applied the same 70 ps, 820 nm laser pulses, at a reduced fluence of 1 mJ cm^{-2} in a multi-pulse mode (at 40 Hz repetition rate) to heat NPs without PNB generation. Cumulative effect of multiple pulses determined the optical dose and corresponding effect of hyperthermia. The cell death level was analyzed after 72 hours. Minimal cancer cell death (about 2±2 %) was detected for optical dose of 24 J cm^{-2} (10 min exposure). Transient heating of individual target cells was monitored in real time through their time-responses and did not show any detectable heating at this fluence. After increasing the optical dose to 144 J cm^{-2}, we observed 20% cancer cell death but the death level among normal cells was similar. Efficient thermal destruction of cancer cells (Fig. 3B) was only achieved after increasing the incubation concentration of NPs by five times at an optical dose of 24 J cm^{-2}. No cells were killed outside the laser beam. However, 91±8 % of normal cells were killed compared to 63±12% of cancer cells (Table S1).

For the higher NP concentration, the time-response of cancer cells showed the typical heating-cooling shape (Fig. 2B, insert)[13]. Using the 200 ns duration (t) of the tail of this time-response from a single pulse, we estimated the diameter (D) of the spherical volume heated through thermal diffusion from gold NPs[7] to be ~ 2 μm ($D = 12*[t*\alpha]^{0.5}$, assuming the thermal diffusivity, α, of the cell was that of water, ~ 1.4×10^5 μm^2 sec^{-1}). This exceeded the size of a NP cluster, but was small compared to a cell diameter. For continuous optical excitation for 100 s and longer, the heated zone increases to a millimeter diameter volume that precludes single cell selectivity. However, even under pulsed excitation, the therapeutic selectivity was low and was determined by the size of the laser beam (Fig. 2B III). Normal cells were destroyed by the thermal impact of non-specifically coupled NPs due to the high targeting concentration.

To evaluate combining chemotherapy with PNBs, free cisplatin and doxorubicin and liposome-encapsulated doxorubicin (Doxil) were applied to the same co-culture prior to PNB generation (Fig. 2C). Fig. 3B shows the death level among cancer and normal cells measured after 72 hours of continuous drug exposure as a function of drug concentration. Our results confirmed the drug-resistance of OCSCC cells (Table S1): cancer cell death levels were lower than normal cells at all concentrations (Fig. 2C, 3B). Next, we applied PNBs of variable lifetimes (sizes) while the cells were exposed to drugs. Compared to the drugs or PNB alone, the death level for cancer cells increased by 25 times for cisplatin, 6 times for doxorubicin and 33 times for Doxil, while the death level remained low among normal cells (Fig. 3B, Table S1). Observed enhancement of cancer cell death was achieved at 10-fold reduced drug concentrations (Fig. 3B): 2 μg ml^{-1} for Cisplatin, 5 μg ml^{-1} for Doxorubicin and 20 μg ml^{-1} for Doxil. Similar cell death levels for the drugs alone required an order of magnitude higher drug dose (20 μg ml^{-1} for cisplatin, 50 μg ml^{-1} for doxorubicin and 200 μg ml^{-1} for Doxil). Reduced drug doses together with a lower laser fluence required to initiate effective PNBs in cancer cells (Table S1) resulted in a significant reduction of non-specific toxicity for the combination treatment (Fig. 3B, Table S1). Fig. 3C–E shows the increased efficacy and selectivity of the combined drug/PNB treatment compared to either PNB or drugs alone, which was maximized for liposome-encapsulated doxorubicin (Doxil, Fig. 3E). Doxil required the minimal PNB lifetimes (28±5 ns) to achieve high level of cell death, while free Doxorubicin required larger PNBs with lifetimes up to 90 ns to achieve similar therapeutic effect (Fig. 3D).

The lifetime of PNBs generated under identical conditions in normal cells was close to zero and varied from 1±1 ns for Doxil to 9 ±5 ns for doxorubicin (Table S1). Such small PNBs did not enhance the chemotherapeutic effects of the drugs and did not kill normal cells (Fig. 3C–E). Such high selectivity of PNB/drug treatment was provided by endocytotic targeting of the NP conjugates that led to a greater probability of NP cluster formation in cancer cells, resulting in preferential PNB generation and increased lifetime. It is important to note that these results were achieved by single broad laser pulse irradiation of large number of normal and cancer cells in co-culture (red circles in Fig. 2A,B). Among the three drugs studied, the PNB-Doxil combination required the minimal PNB lifetime to destroy cancer cells (65 ns) and hence minimal optical fluence, and provided the lowest non-specific toxicity (normal cell death level below 15%).

We further explored the effect of PNB/Doxil by increasing the number of laser pulses from 1 to 4, and by removing Doxil from cells immediately after the PNB treatment (thus reducing exposure from 72 hours to minutes). Increasing the number of PNB treatments from one to four improved cancer cell death level by 1.5 times (Fig. 3F) while the normal cell death level remained at 4%. The immediate removal of Doxil after the PNB treatment slightly reduced cancer cell death level (Fig. 3F). However, the level of cell death after removing the drug was still 1.4 times higher than the sum of the death levels obtained in PNB only and drug only modes (Fig. 3F). Consequently, the combined PNB/Doxil treatment can significantly shorten drug exposure to reduce non-specific toxicity. In all experiments, cell death level correlated to PNB lifetime (Fig. 3A) which correlates to the PNB size. The PNB size, in turn, was determined by the fluence of laser pulse (Fig. S2D,E). Therefore, PNB lifetime can be considered as a metric of the therapeutic effect and can be used to guide and adjust the laser fluence to the level that provides the desired PNB lifetime.

The described above enhancement of selectivity and efficacy of PNB/drug therapy was achieved through two mechanisms: 1) the selective generation of PNBs primarily in cancer cells via the formation of NP clusters due to the enhanced endocytocis due to antibody targeting; and 2) PNB-induced transient permeation of the extracellular drug through the cellular membrane (due to the perforation, stretching or other mechanically-enhanced permeability of the membrane) (Fig. 1C). By supplementing passive drug diffusion through the cell membrane by “active injection” the amount of drug delivered into the cytoplasm is increased and the time required for drug exposure is reduced to as little as a fraction of a second. Based on our previous results,[9] we estimated the delivered volume of 10^{-12} ml, which corresponds to $10^{-17–18}$ g of doxorubicin per cell. The rapid increase in drug level along with the mechanical damage to the cell by the PNB provides a synergistic effect in cell destruction (Fig. 3C–E): the cell death level in the combined PNB/drug mode exceeded the sum of the death levels for PNB-alone and drug-alone modes by 1.7 times for cisplatin, 1.4 times for doxorubicin and 3.5 times for Doxil. The increased advantage for the liposome encapsulated Doxil is two-fold: (1) minimal drug release occurs in cells without PNB (i.e. normal) cells; (2) the delivered amount of encapsulated doxorubicin (estimated at 10^{-16-17} g) was greater than for the free doxorubicin. Specific mechanisms of PNB-induced disruption and release of molecular cargo from liposomes and of intracellular delivery of molecular cargo were verified earlier by us.[9, 16]

The major limitation of this combined therapy is that both NPs and optical energy must be delivered to the target cells. NP delivery is complicated by non-specific uptake by normal cells. For superficial cancers, local delivery in the form of topical application or injection of NPs 24 hours before laser treatment should provide the best result. Unlike using NP for hyperthermia, NP delivery for PNB generation requires much smaller loads, which simplifies delivery and improves safety.

Controlled propagation of optical radiation in deep tissue is the second limiting issue: even in the safest and transparent near-infrared window,[17] laser radiation can be controlled only to a maximum depth of a few millimeters.[18] This means that the ideal PNB target should be thin and superficial. Optical doses for the PNB-chemotherapy combination were 20–40 mJ cm^{-2}, which is within FDA safety limits for living tissues[19] and is significantly lower than the optical doses associated with other photothermal therapies.[5] Larger areas (cm^2) can be treated by scanning the laser in a similar fashion to commercial picosecond near-infrared laser and fiber optic equipment employed in laser surgery. The heterogeneity of NP cluster size and the necessary optical fluence can be dynamically compensated by using the optical and acoustic signals of PNBs (that characterize their size) as feedback in an automated algorithm for control of the laser energy. As the PNB therapeutic mechanism requires a single event, such feedback can efficiently maintain the required PNB size. We recently described a theranostic algorithm[12] that can support such minimally invasive combined treatment.

Chemotherapy has been enhanced with other methods that use ultrasound and laser radiation,[20] which employ thermal and/or mechanical effects similar to PNBs. However, the selectivity is low since these methods cannot discriminate between cancer and normal cells. NP-induced photothermal methods are similar to bulk hyperthermia-enhanced chemotherapy,[21] which has been reported to overcome drug resistance.[22] Gold NP-mediated hyperthermia has been applied in combination with chemotherapy;[23] improvements in efficacy are ascribed to a not fully understood or controlled permeabilization of cellular membranes which facilitates drug uptake. Other studies reported that hyperthermia resulted in opposite effects, inducing drug resistance[24] and/or increased thermo-tolerance of cancer cells.[23, 25] Even with actively-targeted gold nanoparticles, the selectivity of hyperthermia is low due to high NP loadings, unavoidable non-specific coupling of NPs to normal cells,[4, 5] and the associated non-specific toxicity due to heat diffusion to normal cells (Fig. 3B). As we showed here (Table S1), heat generation and diffusion is a cumulative process that cannot differentiate between NP clusters in cancer cells and the single NPs in normal cells. Finally, the cumulative optical doses required for nano-hyperthermia[4, 5] are 3–6 orders of magnitude higher (10 – 10000 J cm^{-2}) than the optical doses required for PNB therapy (10 – 40 mJ cm^{-2}). Combined hyperthermia-drug approaches suffer from 1) long treatment times, 2) low selectivity and high non-specific toxicity, 3) high optical doses and 4) multiple biological mechanisms that complicate therapy.

The combined PNB-drug mechanism of cell destruction described in this communication 1) acts fast (nanoseconds) via a single, externally-controlled laser pulse, 2) uses localized mechanical processes (cell permeation and drug delivery), instead of a diffusive thermal process, 3) requires low NP loads and optical doses, and 4) allows for real time feedback and guidance. These factors combine to provide the high selectivity and efficacy of the PNB-drug therapy. Recently, more complex NPs have been synthesized that carry both a cell specific targeting agent, gold NPs and a drug[10, 26] and to deploy the drug upon optical activation of the gold NPs. However, such complex NPs are difficult to synthesize, must be engineered for each application, they can be unstable *in vivo* and their unavoidable non-specific uptake by normal cells may increase non-specific toxicity and may reduce therapeutic selectivity.

To conclude, we compared three modes of the cell level delivery of therapeutic effect with gold NPs, hyperthermia (thermal), plasmonic nanobubbles (mechanical) and a combination of drugs with plasmonic nanobubbles (chemotherapeutic). Among all three the combination of plasmonic nanobubbles with standard anti-cancer drugs demonstrated the best effect as a

proof of principle for a novel nano-therapeutic mechanism for selective, efficient, safe and guided treatment of drug-resistant superficial cancer:

1. Selective intracellular delivery of standard extracellular drugs via laser-induced PNBs overcomes drug- and thermal- resistance of cancer cells.
2. A high therapeutic selectivity is achieved through cancer cell targeting with specific antibody conjugates of gold NPs and their intracellular clustering which allowes for cell-specific generation of PNBs under excitation with broad laser beams in single pulse mode at a physiologically safe level of laser radiation.
3. Drug doses required for total destruction of OCSCC cells are reduced by an order of magnitude, while non-specific toxicity is reduced to 15% of death level among normal cells and the treatment time required is reduced from days to minutes.

Supplementary Material

Refer to Web version on PubMed Central for supplementary material.

Acknowledgments

Authors thank Dr. Gary Braun of the University of California, Santa Barbara, Andrey Belyanin of Rice University for their generous help in synthesis of hollow gold nanoshells, Hannie and Glenn Ford, PhD of BioAssayWorks LLC (Ijamsville, MD) for their help in the conjugation of gold nanoparticles, Drs. Dan Carson and Mary C. Farach-Carson for helpful discussions at “nanobubbler” seminars at Rice University, Ms. Shruti Kashinath for her help with cell culturing and Ms. Susan Parminter for copy-editing the manuscript. This work was supported in part by National Institute of Health Grants R01GM094816 (DOL) and RO1EB012637 (JAZ). Confocal microscopy was performed on equipment obtained through a Shared Instrumentation Grant from the National Institutes of Health (S10RR026399-01).

References

[1]. Jemal A, Siegel R, Xu J, Ward E. CA Cancer J. Clin. 2010; 60:277. [PubMed: 20610543]

[2]. Ow TJ, Myers JN. Clin. Exp. Otorhinolaryngol. 2011; 4:1. [PubMed: 21461056]

[3]. a) Cho K, Wang X, Nie S, Chen ZG, Shin DM. Clin. Cancer Res. 2008; 14:1310. [PubMed: 18316549] b) Peer D, Karp JM, Hong S, Farokhzad OC, Margalit R, Langer R. Nat. Nanotechnol. 2007; 2:751. [PubMed: 18654426] c) Meng H, Liong M, Xia T, Li Z, Ji Z, Zink JI, Nel AE. ACS Nano. 2010; 4:4539. [PubMed: 20731437] d) Liang XJ, Meng H, Wang Y, He H, Meng J, Lu J, Wang PC, Zhao Y, Gao X, Sun B, Chen C, Xing G, Shen D, Gottesman MM, Wu Y, Yin JJ, Jia L. Proc. Natl. Acad. Sci. U S A. 2010; 107:7449. [PubMed: 20368438]

[4]. a) Cai W, Gao T, Hong H, Sun J. Nanotechnology, Science and Applications. 2008; 1:17.b) Boisselier E, Astruc D. Chem. Soc. Rev. 2009; 38:1759. [PubMed: 19587967] c) Sokolov K, Follen M, Aaron J, Pavlova I, Malpica A, Lotan R, Richards-Kortum R. Cancer Res. 2003; 63:1999. [PubMed: 12727808] d) Pitsillides CM, Joe EK, Wei X, Anderson RR, Lin CP. Biophys. J. 2003; 84:4023. [PubMed: 12770906]

[5]. a) El-Sayed IH, Huang X, El-Sayed MA. Nano Lett. 2005; 5:829. [PubMed: 15884879] b) Loo C, Lowery A, Halas N, West J, Drezek R. Nano Lett. 2005; 5:709. [PubMed: 15826113] c) West JL, Halas NJ. Annu. Rev. Biomed. Eng. 2003; 5:285. [PubMed: 14527314]

[6]. a) Cherukuri P, Glazer ES, Curley SA. Adv. Drug. Deliv. Rev. 2010; 62:339. [PubMed: 19909777] b) Kennedy LC, Bickford LR, Lewinski NA, Coughlin AJ, Hu Y, Day ES, West JL, Drezek RA. Small. 2011; 7:169. [PubMed: 21213377]

[7]. Lapotko D. Opt. Express. 2009; 17:2538. [PubMed: 19219157]

[8]. Lukianova-Hleb E, Lapotko DO. Nano Lett. 2009; 9:2160. [PubMed: 19374436]

[9]. Lukianova-Hleb EY, Samaniego AP, Wen J, Metelitsa LS, Chang CC, Lapotko DO. J. Control. Release. 2011; 152:286. [PubMed: 21315120]

[10]. Braun GB, Pallaoro A, Wu G, Missirlis D, Zasadzinski JA, Tirrell M, Reich NO. ACS Nano. 2009; 3:2007. [PubMed: 19527019]

[11]. Lapotko D, Lukianova E, Potapnev M, Aleinikova O, Oraevsky A. Cancer Lett. 2006; 239:36. E. Y. Lukianova-Hleb, Koneva, II, A. O. Oginsky, S. La Francesca, D. O. Lapotko, *J. Surg. Res.* **2011**, *166*, e3. [PubMed: 16202512]

[12]. Wagner DS, Delk NA, Lukianova-Hleb EY, Hafner JH, Farach-Carson MC, Lapotko DO. Biomaterials. 2010; 31:7567. [PubMed: 20630586]

[13]. Lukianova-Hleb E, Hu Y, Latterini L, Tarpani L, Lee S, Drezek RA, Hafner JH, Lapotko DO. ACS Nano. 2010; 4:2109. [PubMed: 20307085]

[14]. Lapotko DO, Lukianova-Hleb EY, Oraevsky AA. Nanomedicine (Lond). 2007; 2:241. [PubMed: 17716124]

[15]. Vogel A, Noack J, Huttman G, Paltauf G. Appl. Phys. B-Lasers O. 2005; 81:1015.

[16]. Anderson L, Hansen E, Lukianova-Hleb EY, Hafner JH, Lapotko DO. J. Control. Release. 2010; 144:151. [PubMed: 20156498]

[17]. Weissleder R. Nat. Biotechnol. 2001; 19:316. [PubMed: 11283581]

[18]. Svaasand L. Lasers in Medical Science. 1989; 4:309.

[19]. Laser Institute of America. American national standard for safe use of lasers (ANSI Z136.1–2000). 2000.

[20]. a) Fechheimer M, Boylan JF, Parker S, Sisken JE, Patel GL, Zimmer SG. Proc. Natl. Acad. Sci. U S A. 1987; 84:8463. [PubMed: 2446324] b) Prentice P, Cuschierp A, Dholakia K, Prausnitz M, Campbell P. Nat. Phys. 2005; 1:107.

[21]. a) Hildebrandt B, Wust P, Ahlers O, Dieing A, Sreenivasa G, Kerner T, Felix R, Riess H. Crit. Rev. Oncol. Hematol. 2002; 43:33. [PubMed: 12098606] b) Herman TS, Teicher BA, Jochelson M, Clark J, Svensson G, Coleman CN. Int. J. Hyperthermia. 1988; 4:143. [PubMed: 3283266] c) Kowal CD, Bertino JR. Cancer Res. 1979; 39:2285. [PubMed: 376118]

[22]. Gottesman MM. Cancer Res. 1993; 53:747. [PubMed: 8094031]

[23]. Chan WCW, Hauck TS, Jennings TL, Yatsenko T, Kumaradas JC. Adv. Materials. 2008; 20:3832.

[24]. Fisher B, Kraft P, Hahn GM, Anderson RL. Cancer Res. 1992; 52:2854. [PubMed: 1581899]

[25]. a) Urano M. Cancer Res. 1986; 46:474. [PubMed: 3510074] b) Rege K, Huang HC, Yang Y, Nanda A, Koria P. Nanomedicine. 2011; 6:459. [PubMed: 21542685] c) Lepock JR. Int. J. Hyperthermia. 2003; 19:252. [PubMed: 12745971]

[26]. a) Wu GH, Milkhailovsky A, Khant HA, Fu C, Chiu W, Zasadzinski JA. JAC. 2008; 130:8175.b) Paasonen L, Sipila T, Subrizi A, Laurinmaki P, Butcher SJ, Rappolt M, Yaghmur A, Urtti A, Yliperttula M. J. Control. Release. 2010; 147:136. [PubMed: 20624434] c) Pissuwan D, Niidome T, Cortie MB. J. Control. Release. 2011; 149:65. [PubMed: 20004222] d) Qin G, Li Z, Xia R, Li F, O'Neill BE, Goodwin JT, Khant HA, Chiu W, Li KC. Nanotechnology. 2011; 22:155605. [PubMed: 21389566]

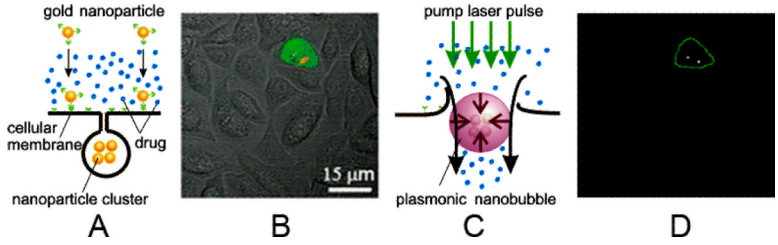

Figure 1.

Principles of plasmonic nanobubble therapies. A: Free drug and gold NP targeting: formation of intracellular clusters of gold nanopartciles (NP) employs antibody-receptor interaction and endocytosis; B: Overlaid fluorescent, scattering and bright field confocal microscopy images of a co-culture of cancer (green) and normal (colorless) cells with clusters of gold NPs (red); C: Generation of plasmonic nanobubble (PNB) through absorption of the pump short laser pulse (green) and follow up transient perforation of the cell, and intracellular injection of the extracellular drug by inbound jet that accompanies the collapse of PNB; D: Time-resolved optical scattering image of transient plasmonic nanobubbles generated in target cell with a single laser pulse that irradiated all shown in B and E (70 ps, 820 nm, 40 mJ cm^{-2}).

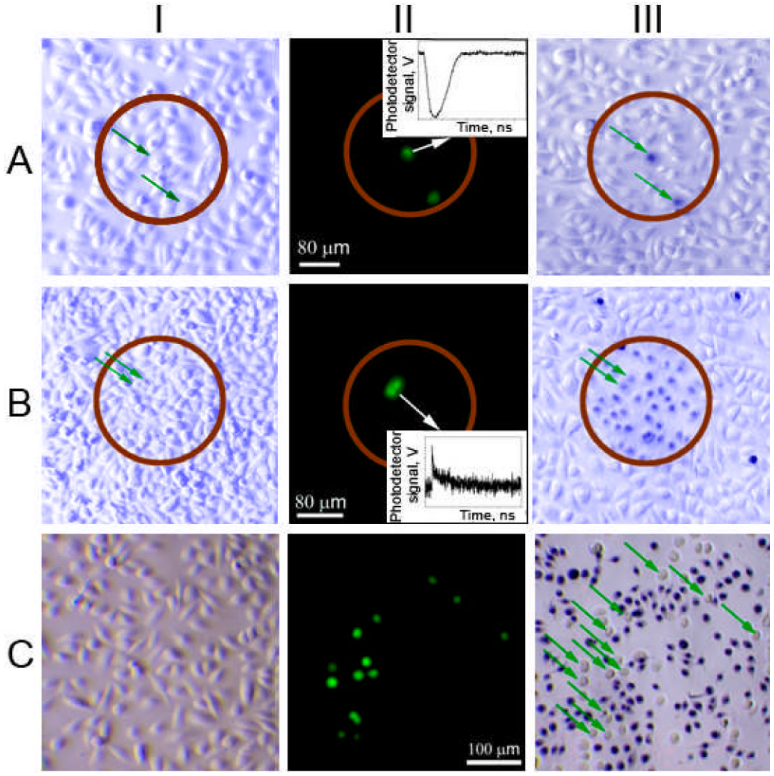

Figure 2.

Bright field (I, III) and fluorescent (II) microscopy images of a co-culture of normal (NOM9) and squamous cell carcinoma (HN31, green or shown with green arrows) cells, the images I and II were taken before treatment and the image III was taken after the treatment and after staining the cells with Trypan Blue (blue - dead cells, white - live cells). A: PNB treatment with a single laser pulse (70 ps, 820 nm, 40 mJ cm^{-2}), the time-response (insert) obtained from one of cancer cells shows a PNB; B: Nano-hyperthermia treatment (NP concentration was 5-fold increased, laser treatment: 40 Hz, 820 nm, 24 J cm^{-2}) the time-response (insert) obtained from one of cancer cells shows a heating-cooling signal; C: Cisplatin (5 μg ml^{-1}) treatment for 72 hours.

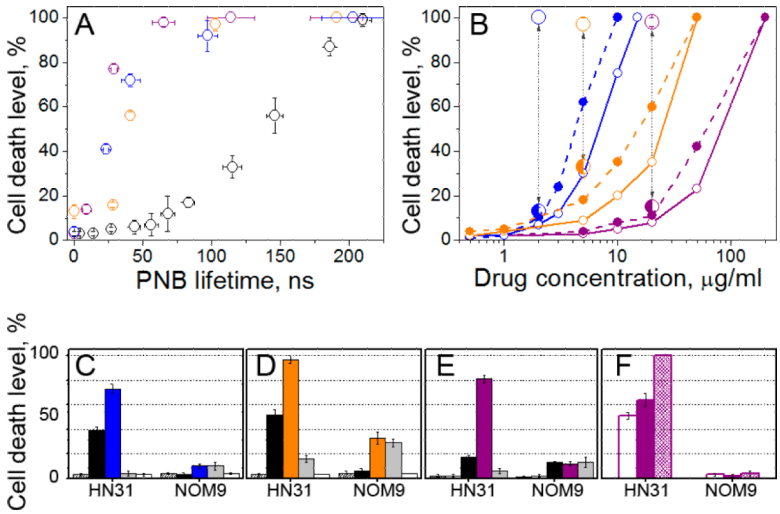

Figure 3.

Comparison of the efficacy and selectivity of PNBs and drugs (black: PNB alone, blue: Cisplatin, orange: Doxorubicin, purple: Doxil) shown through the levels of cell death (72 h) among cancer (HN31, hollow dots) and normal (NOM9, solid dots) cells in a co-culture as function of: A - maximal size of PNB (PNB lifetime), Cisplatin (2 μg ml^{-1}), Doxorubicin (5 μg ml^{-1}), Doxil (20 μg ml^{-1}); B: drug concentration without PNBs (small dots) and with PNBs (large dots) in cancer/normal cells: Cisplatin (90±10/9±5 ns), Doxorubicin (90±10/9±5 ns), Doxil (65±8/11±4 ns); C-E: comparison of the different treatments (grey: drug alone, white: intact cells, dashed: NPs alone), C: Cisplatin, PNB lifetime in cancer/normal cells: 41±7 / 2±5 ns, D: Doxorubicin, PNB lifetime in cancer/normal cells: 90±10 / 9±5 ns, E: Doxil, PNB lifetime in cancer/normal cells: 28±5 / 1±1 ns; F: Doxil and single PNB (purple), Doxil being immediately removed after treatment with single PNB (white), 4 sequential PNBs (dashed).